# Sequential design of computer experiments

**Hugo Maruri-A.♠ with R. Bates♢, A. Boukouvalas♯ P. Curtis♠ and H. Wynn♣**

♠ School of Mathematical Sciences, Queen Mary, University of London
♣ CATS, LSE, ♯ ASTON University, ♢ Rolls-Royce plc


MASCOT NUM 2015
Saint-Étienne 8-10 April 2015

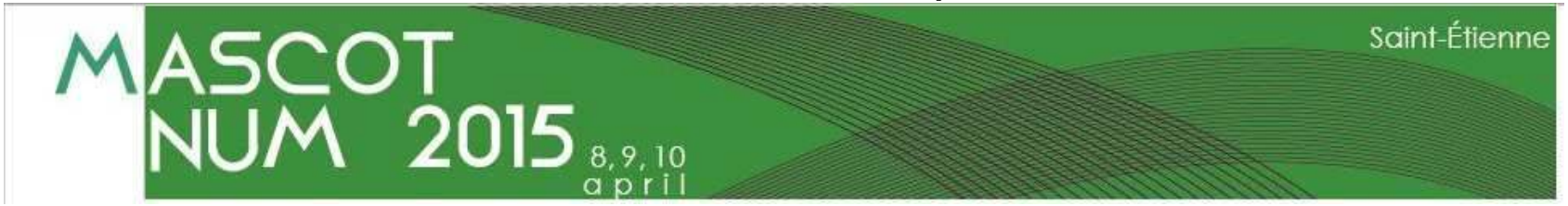

# History matching and implausibility

- Simulation data $y$ is assumed to consist of emulator $f(x)$ plus a discrepancy term $\eta$. This simulation of a physical model is related to observational data $z$ through an error term $e$:

$$z = \underbrace{f(x) + \eta}_{y} + e = y + e.$$

- Implausibility is a measure of the fit of the modelling scheme to real data $z$. For an input value $x_0$, the **implausibility** can be defined as

$$\mathcal{I}(x_0) = (z - E[f(x_0)])^T \left(Var\left(z - E[f(x_0)]\right)\right)^{-1} (z - E[f(x_0)])$$

  High values of implausibility indicate that the model does not agree with data. Low implausibility values are used together with a threshold to define regions which have not been ruled out yet (**NROY**) from the study:

$$\mathcal{X}_{NROY} = \{x \in \mathcal{X} : |\mathcal{I}(x)| \leq a\}.$$

A rule of thumb value for the threshold is $a = 3$, see Williamson and Vernon (2014). When dealing with several output variables, the implausibility is usually computed using a worst-case scenario as the maximum of implausibilities for different outputs.

Starting with an **initial** design over a region of interest $\mathcal{X}$, an emulator is built. Unimportant factors are dropped and so are points which do not match the observed data. This narrows the study, and a **second wave** design is created in a smaller region, a model fitted and implausibility criterion used to update the region $\mathcal{X}_{NROY}$. After a **few waves** we end with a good fitting model and a reduced NROY region.

**Efficient** sampling strategies are important, as the NROY region in subsequent waves is usually small relative to the initial design, and in practice it may become disconnected. Simple, space filling designs often have **low** efficiency when the NROY region is small.

Our proposal is to build a smooth response surface for implausibility $\mathcal{I}(x)$ and exploit it to obtain new design points.

# Smooth supersaturated models (SSM)

We start with a data set $y$ over a design $D$ of $n$ unique points. Write the vector of model terms as $f(x) = (x^\alpha : \ \alpha \in M)^T$ so that

$$\eta(x) = f(x)^T \theta, \tag{1}$$

where $\theta$ is the vector of coefficients for terms in $f(x)$. The set $M$ contains exponents of monomial terms $x^\alpha$; satisfies hierarchy and contains at least one identifiable model. Its size is such that $|M| > n$.

**SSM** The polynomial model

$$Y(x) = \sum_{\alpha \in M} \theta_\alpha x^\alpha \tag{2}$$

is smoothed, subject to interpolation conditions

$$\min \int_{\mathcal{X}} \text{tr}(H(Y)^2) dx \text{ such that } X\theta = y.$$

# Exploting the response surface of implausibility $\mathcal{I}(x)$

We start with a synthetic implausibility function. White area is NROY space, defined when $\mathcal{I}(x) \leq 3$. The search starts with values of $\mathcal{I}(x)$ less than five (purple area indicates values s.t. $3 < \mathcal{I}(x) < 5$).

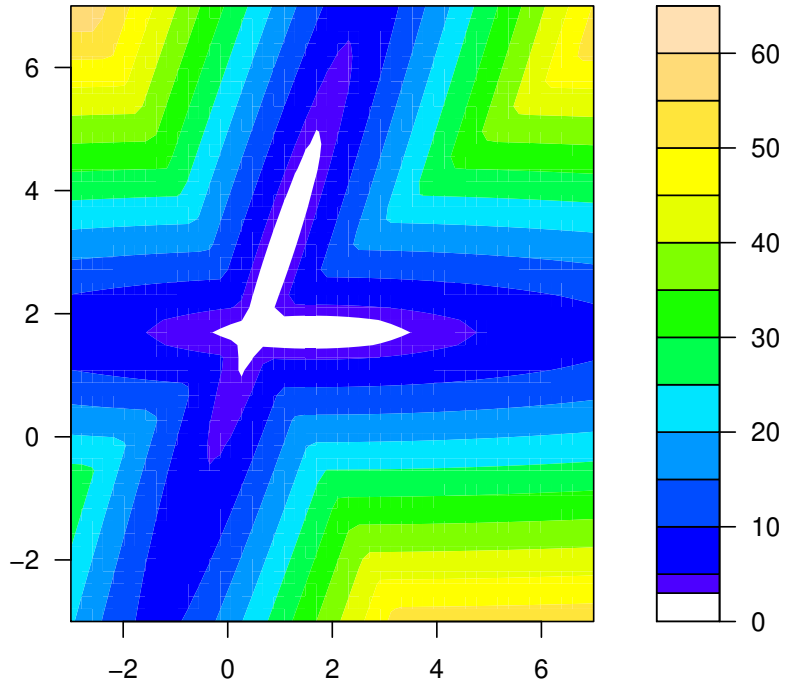

# Wave one: initial fit and locating potential minima

Using $50$ design points, a smooth polynomial emulator is produced using $400$ smoothing terms. The black dot indicates a local minimum of the emulator surface, which will be used as starting point.

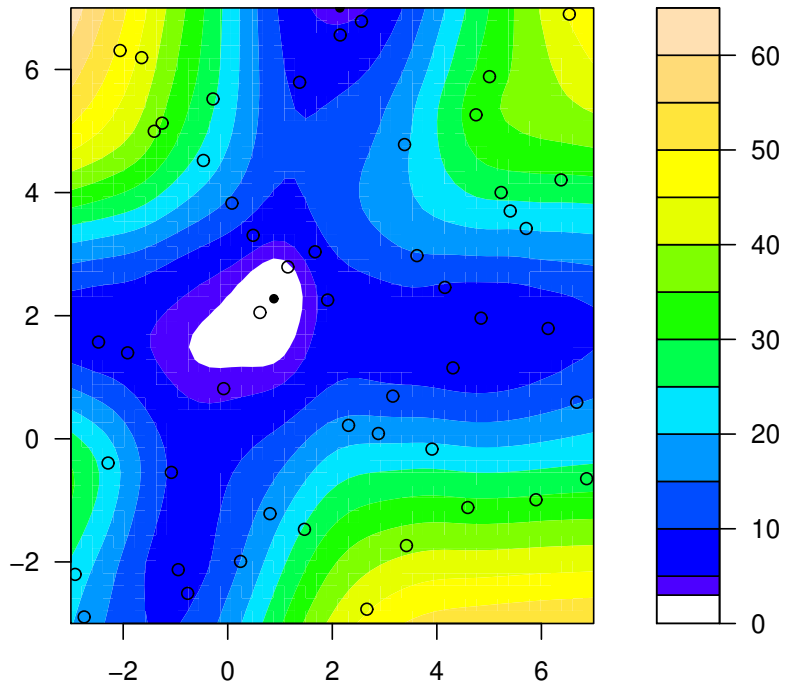

# The cone method (Bates et al 2007)

The method assumes that the region of interest is star-shaped around the central point. Starting from a (suspected) central point, the cone method generates candidate points in different directions.

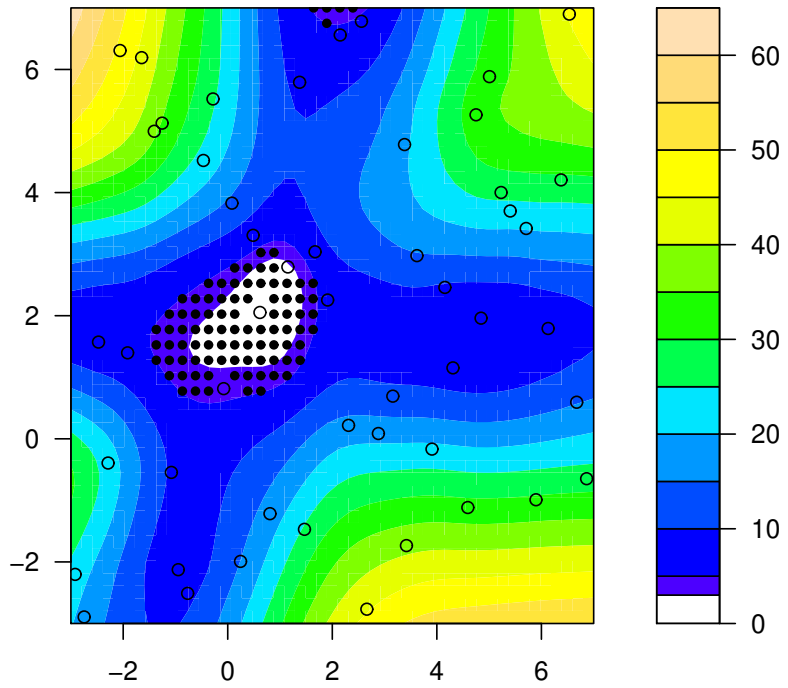

# Selecting new candidate points for wave two

The lattice points from the cone method can be used for the next wave. In this case, we wanted only ten new points. These were selected randomly from ten clusters formed from the lattice points.

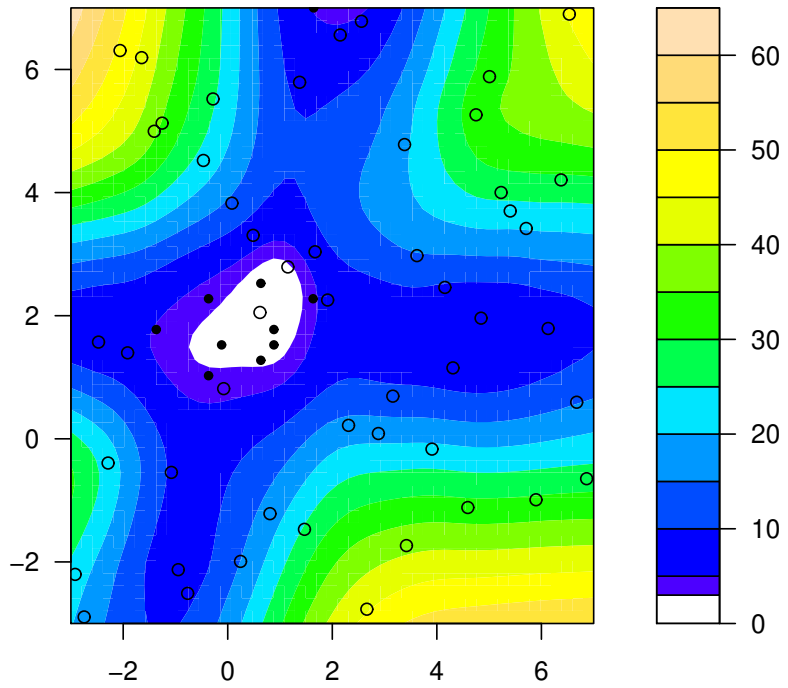

At this stage, only one of this wave of ten points is in NROY and five points have implausibility below five. This is not entirely surprising as there must be some burn in.

We progress to **wave 2** and the new SSM shows the NROY region slowly forming.

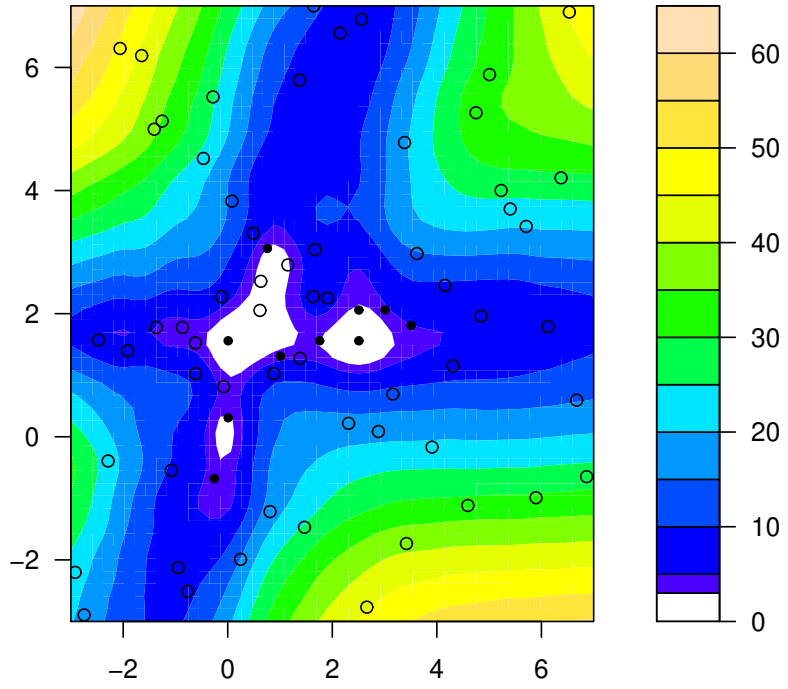

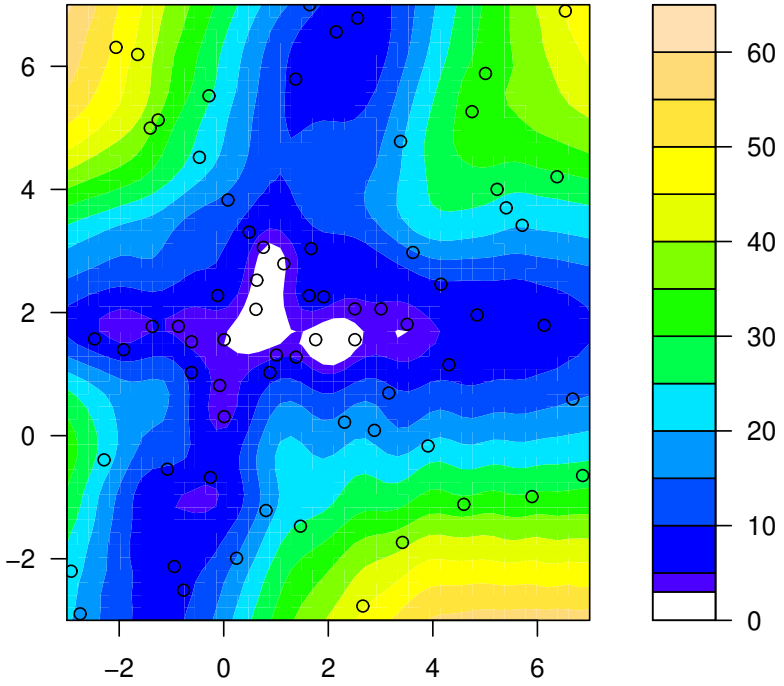


In **wave 3**, only two of the points generated are within NROY and six points have implausibility less than five.
Not all points in waves 1-3 are shown, but there is heavy clustering of points in the search area. A global implausibility model for the whole region might not be appropriate and local models might be required.

# Case study: transport data set

We used a simplified version of the microsimulation model described in Boukouvalas *et al.* (2014). Three variables `Headway`, `CarFamiliarity` and `MotorwayCost` were allowed to vary, and nine locations could be selected. The implausibility threshold was $a = 14.9$.

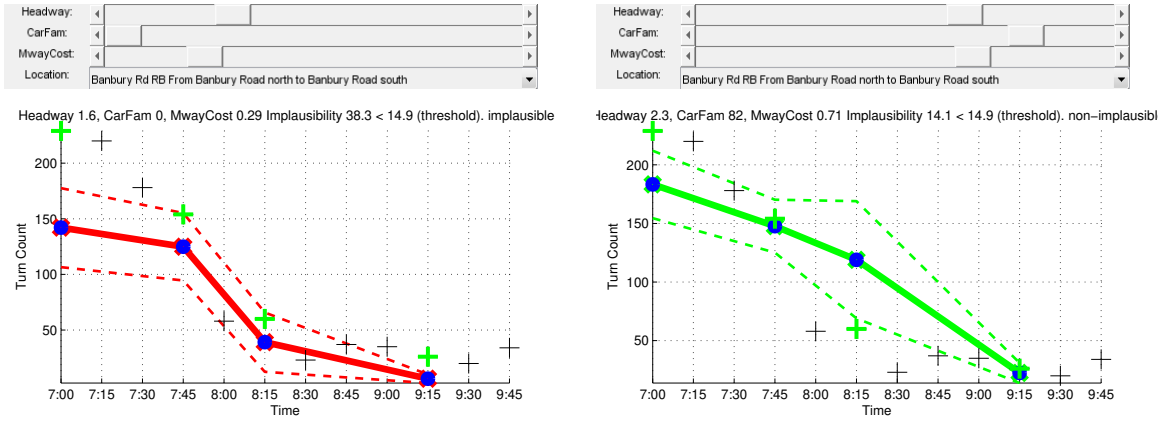


Implausible (left) and non-implausible (right) configurations.

One step (one wave) application of the methodology described using SSM produced efficiency of $60\%$. As a comparison, simple uniform random sampling has an efficiency of $1\%$.

# Comments and future challenges

- Moving around the smooth implausibility surface is very easy as it is polynomial in nature. Gradients are computed instantly and evaluation of response surface is instantaneous.
- Our proposal can be quite efficient in one wave steps
- however it requires a lot of manual intervention if it is to be applied in subsequent waves.
- We want to compare the performance of our method against the implausibility-driven random walk of Williamson and Vernon (2014).

# A closer look at Smooth supersaturated models

## Computing effects

All effects, marginal and interactions have closed formulæ, e.g. the general form for $f_i$, the main effect for the $i$-th factor, is

$$f_i = \int y(x) dx_{-i} - f_0 = \sum_{\alpha \in M} \theta_\alpha \left( \frac{x_i^{\alpha_i}(\alpha_i + 1) - 1}{\prod_{j=1}^{d}(\alpha_j + 1)} \right).$$

The variations of effects have also closed form. For example, the variation of main effect $x_i$ is

$$D_i = \int f_i^2 dx_i = \theta^T \left( \frac{1}{\prod_{j=1}^{d}(\alpha_j + 1)(\beta_j + 1)} \cdot \frac{\alpha_i \beta_i}{\alpha_i + \beta_i + 1} \right)_{\alpha, \beta \in M} \theta.$$

# Engine emissions data (Bates et al., 2003)

This data was collected for the analysis of an engine emissions simulator. One response was available as a function of five input factors. Training data has $48$ observations and validation data set has $49$ observations.

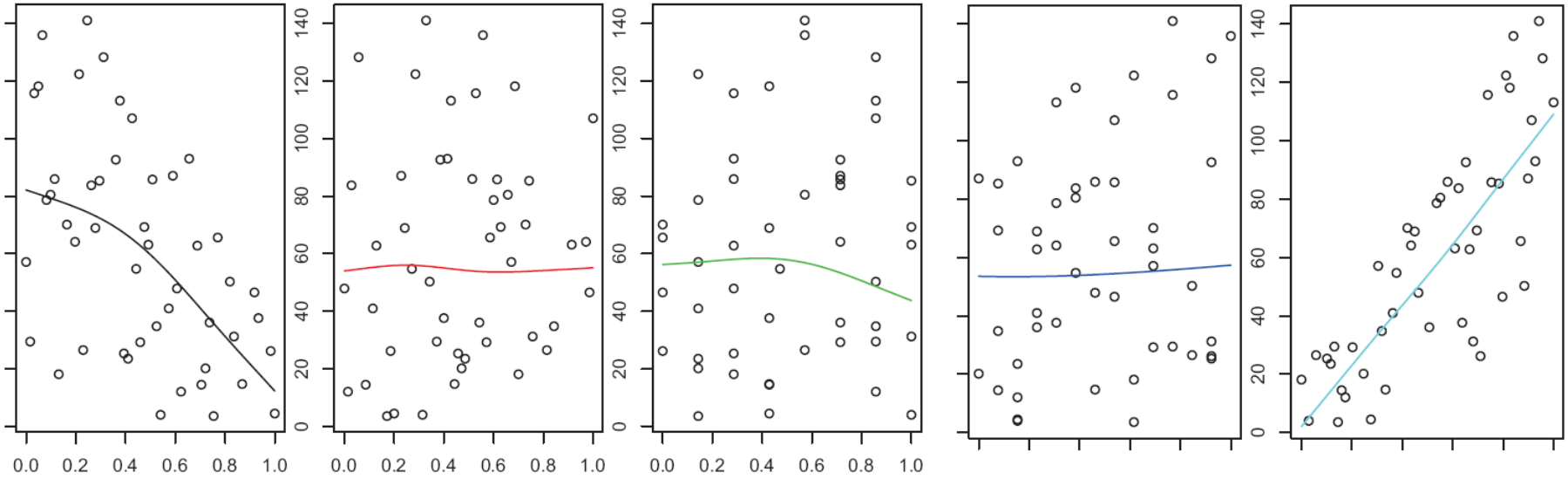


Main effects $(N, C, A, B, M)$, engine emissions data set.

A supersaturated model was fit with $50$ extra terms. The validation RMSE was $6.5$, within $5\%$ of the data range.

# Engine emissions data 2

- Total variance $D = 1494.54$.
- Global sensitivity indices $(\%)$

| Univariate Total $= 97.93\%$ | | | | | Double interactions Total $= 1.58\%$ | | | | | | | | | |
|---|---|---|---|---|---|---|---|---|---|---|---|---|---|---|
| $S_N$ | $S_C$ | $S_A$ | $S_B$ | $S_M$ | $S_{NC}$ | $S_{NA}$ | $S_{NB}$ | $S_{NM}$ | $S_{CA}$ | $S_{CB}$ | $S_{CM}$ | $S_{AB}$ | $S_{AM}$ | $S_{BM}$ |
| 32.68 | 0.12 | 1.04 | 0.16 | 63.90 | 0.06 | 0.13 | 0.36 | 0.56 | 0.07 | 0.01 | 0.03 | 0.02 | 0.09 | 0.20 |

- Main effects: $M$ and $N$. Other: $A$ and $MN$ (small).

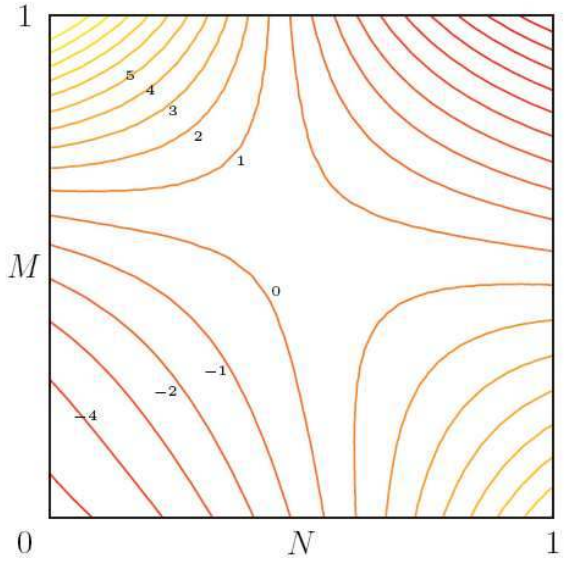


Interaction plot of main effects

# Borehole model (Morris et al., 1993)

This model quantifies waterflow in two aquifers. Its output $y$ is flow rate through the borehole, which depends on eight input parameters.

$$y = \frac{2\pi T_u (H_u - H_l)}{\ln(r/r_w)\left(1 + \frac{2LT_u}{\ln(r/r_w) r_w^2 K_w} + \frac{T_u}{T_l}\right)}$$

Six of the model inputs are kept fixed so that the model depends only on two of the input parameters, termed $t_1 = r_w$ and $t_8 = K_w$.

The design consisted of the following (coded) design points $(0, 0), (0.268, 1)$ and $(1, 0.268)$. At each design site, model response $y$ and partial derivatives with respect to the two inputs $\partial y/\partial t_1$ and $\partial y/\partial t_8$ were evaluated. A smooth Hermite interpolator with $25$ (graded) terms was fitted to the data. The value of smoothness achieved was $\Psi_2^* = 46243.2$.

# Borehole model: results

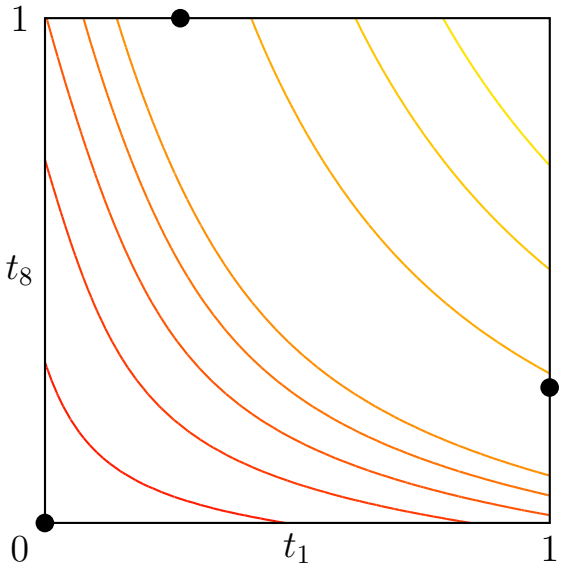


Predicted output $\hat{y}$

Contours: 0,10,20,30,40,50,100,150,200

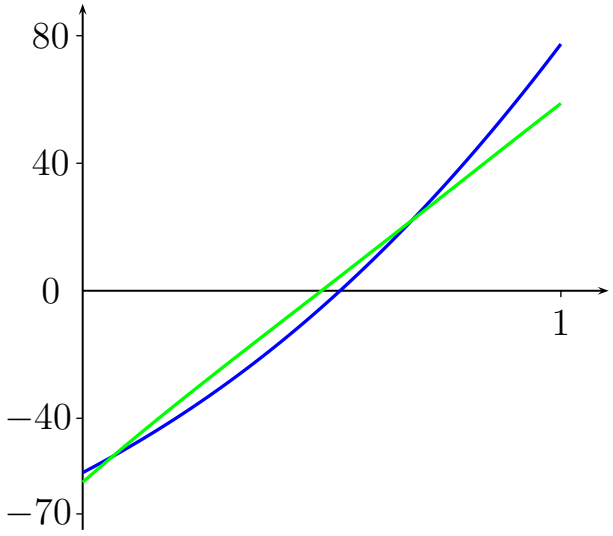


Main effects plot

$f_{t_1}$ and $f_{t_8}$

| Effect | $S_i$ |
|---|---|
| $f_{t_1}$ | 47.44 |
| $f_{t_8}$ | 36.37 |
| $f_{t_1 t_8}$ | 16.19 |

Sobol' indices

Total variation

$D = 3180.3$

# Dependence of $\Psi_2$ on number of extra terms

Smooth supersaturated models have a close relation with (cubic) splines, as splines minimize the criterion $\Psi_2$ (Halliday, 1957). We have observed experimentally that SSM tends to splines as the number of terms used for smoothing increase.

| Extra terms | $0$ | $1$ | $2$ | $3$ | $4$ | $5$ | Spline |
|---|---|---|---|---|---|---|---|
| $\Psi_2^*$ | 76.543 | 74.698 | 33.153 | 33.020 | 27.767 | 27.745 | 26.744 |

Convergence of minimal roughness $\Psi_2^*$ to spline, one dimensional simulated data.

In a multivariate setting, we observe reduction of smoothness $\Psi_2$ as extra terms are introduced. There is no unique way of adding the extra terms and we currently investigate different forms of doing it.

# Engine emissions data 3

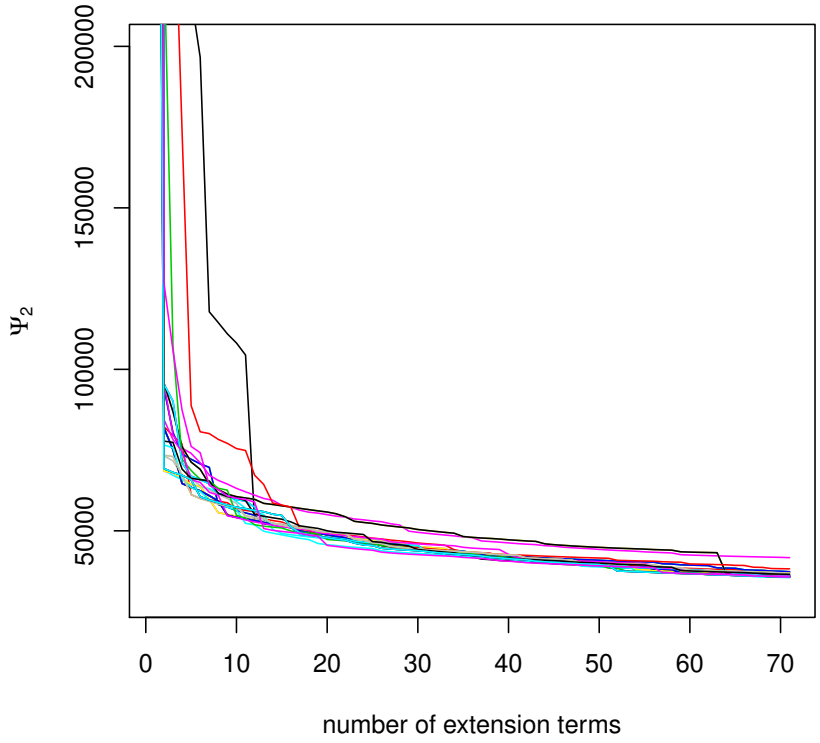


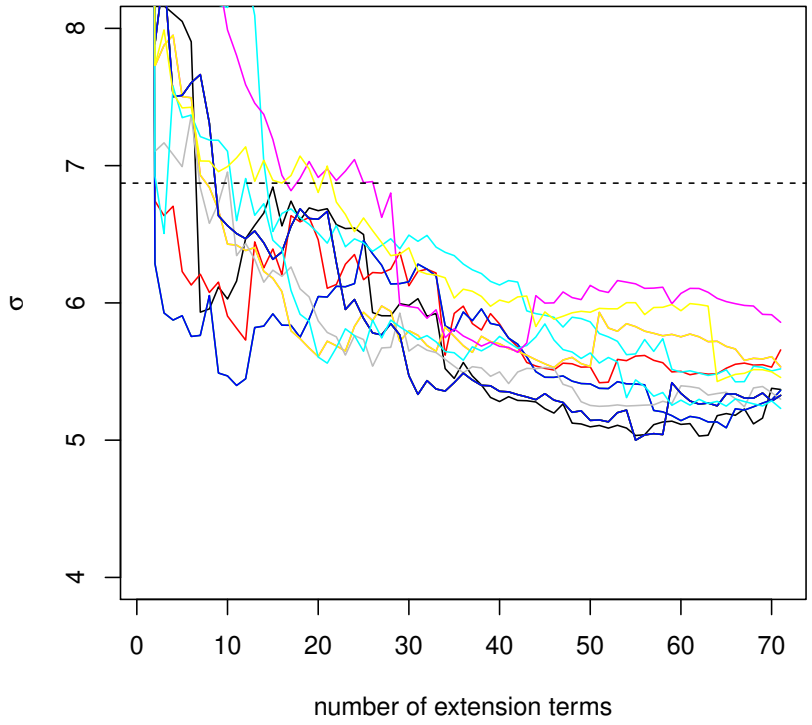


Each trajectory is created from a starting model and sequentially adding terms that minimize $\Psi_2$.

# Engine emissions data 4

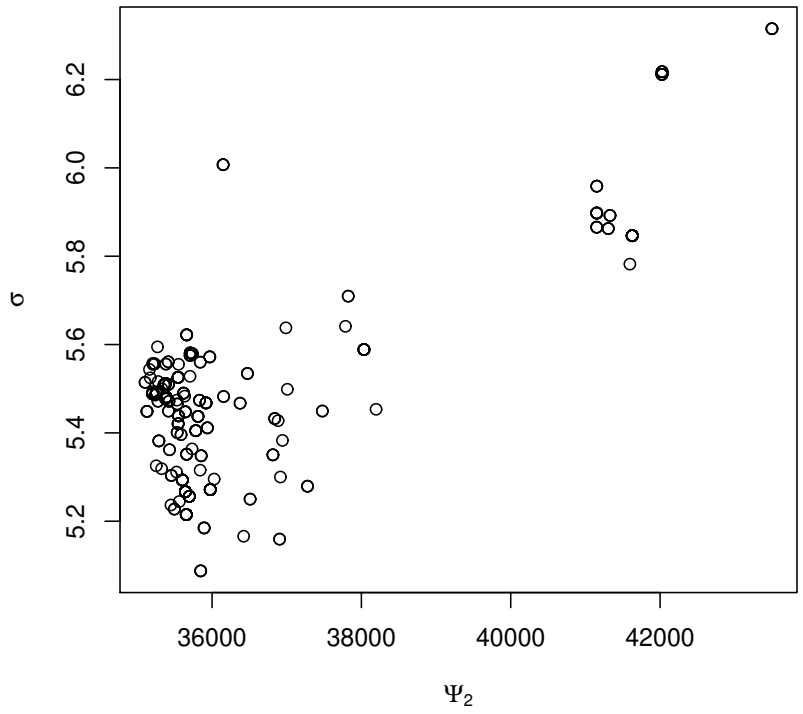


RMSE (using validation data) vs. $\Psi_2$. Each point corresponds to a smooth supersaturated model.

# Smooth supersaturated models and its norm

The smooth model minimizes $\Psi_2$ subject to interpolation conditions. Univariate version of criterion is $\Psi_2 = \int \left(y(x)''\right)^2 dx$.

For functions $f, g$, define inner product

$$\langle f, g \rangle := \int f'' g'' dx = \int \sum_{i,j} f^{ij} g^{ij} dx$$

We are interested in polynomial functions for which $\langle f, g \rangle \geq 0$. Considering monomial terms only, the inequality is strict if we exclude the constant and linear terms in which case $\langle 1, \cdot \rangle = \langle x, \cdot \rangle = 0$.

Now consider $y(x) = f(x)^T \theta$ and the criterion simplifies to

$$\Psi_2 = ||y(x)||^2 = \langle f(x)^T \theta, f(x)^T \theta \rangle = \theta^T \langle f(x), f(x)^T \rangle \theta = \theta^T K \theta$$

with $K := \langle f(x), f(x)^T \rangle$.

# The inner product and representer

We use $\langle \cdot, \cdot \rangle$ to recover functions as $\langle R(s,x), f(x)^T\theta \rangle = f(s)^T\theta$. The representer $R(s,t)$ we build from the inner product is nonparametric

$$R(s,t) = f(s)^T K^{-1} f(t) = f(s)^T \langle f(x), f(x)^T \rangle^{-1} f(t),$$

and only depends on the number of monomial terms involved

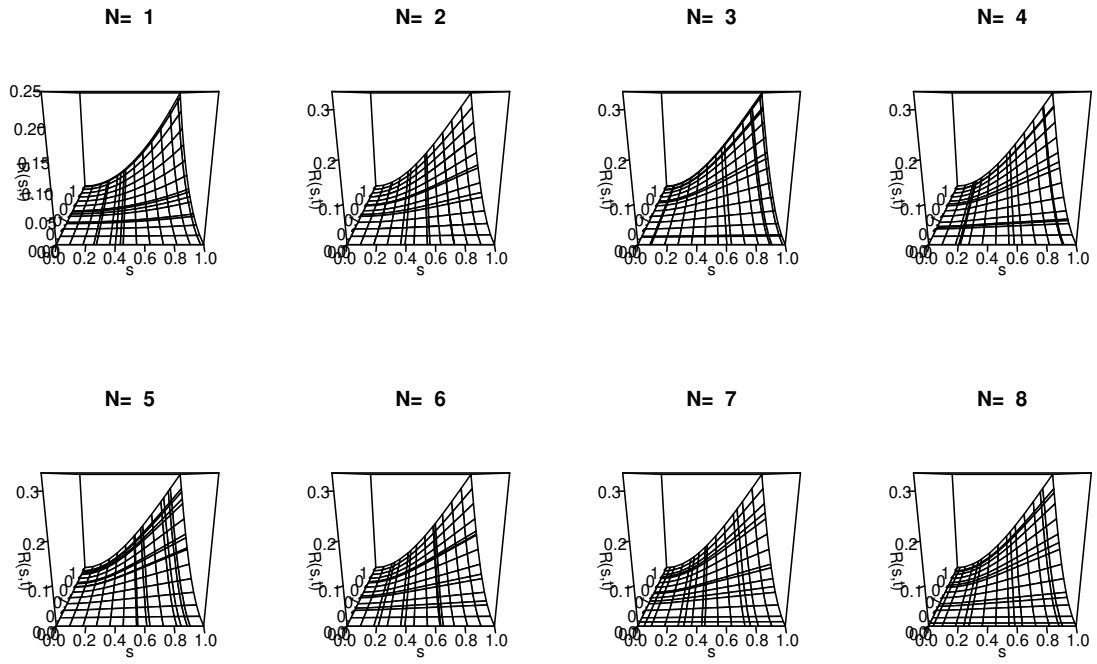

# Eigendecomposition of $R(s,t)$

We decompose $K^{-1} = U^T U$ and with its eigenvalues let $\Lambda = \text{diag}(\lambda_1, \ldots, \lambda_N)$ so that $R(s,t) = f(s)^T K^{-1} f(t) = g(s)^T \Lambda g(t)$, i.e.

$$R(s,t) = \underbrace{f(s)^T U^T \Lambda^{-1/2}}_{g(s)^T} \Lambda \underbrace{\Lambda^{-1/2} U f(t)}_{g(t)} = \sum_{i=1}^{N} \lambda_i g_i(s)^T g_i(t).$$

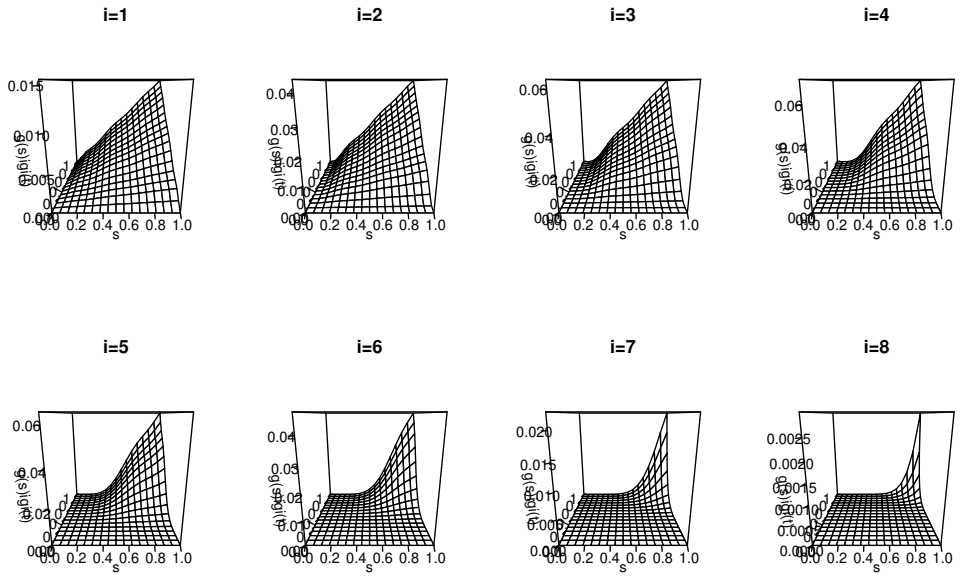

# Final comments and future challenges

- We have developed a methodology which produces model arbitrarily close to splines. We estimate error using validation.
- The methodology allows use of derivative information and it is easy to exploit as a response surface.
- Simple proof of convergence to splines (Bates et al, 2014).
- New developments allow formalization of material in Sobolev spaces, we have given representer $R(s,t)$. Further properties of the representer to be explored.
- Model using representer $y(x) = \theta_0 + \theta_1 x + \sum_{i=1}^{n} \beta_i R(x, x_i)$ potentially more efficient without need to invert large matrix $\begin{pmatrix} X & 0 \\ K & -X^T \end{pmatrix}$ currently at the core of the method.

# References


- **Bates, Maruri-Aguilar, Wynn** (2013). Smooth supersaturated models. *JSCS*.
- **Bates, Curtis, Maruri-Aguilar, Wynn** (2013). Optimal design for smooth supersaturated models. *JSPI*.
- **Bates, Wynn, Fraga** (2007). Feasible region approximation. Eng. Opt. 39(5), 513–527.
- **Boukouvalas, Sykes, Cornford, Maruri-Aguilar** (2014). Bayesian calibration and parameter sensitivity in a stochastic simulation model. *IEEE TITS*.
- **Morris, Mitchell, Ylvisaker** (1993). *Techno.* **35**(3),243-255.
- **Williamson, Vernon** (2014) Efficient uniform designs for multi-wave computer experiments. `arXiv:1309.3520v1`